NUMERICAL AND EXPERIMENTAL STUDY OF FLOW IN SMALL WIND TUNNEL TEST SECTION OPERATING WITH LOW SPEED

Soares, Cleide Barbosa, cleide_bsoares@hotmail.com
Federal Center of Technological Education of Minas Gerais-CEFET-MG, Av. Amazonas, 5.253 – Nova Suiça - Belo Horizonte, Minas Gerais, Brazil- Cep. 30480-000

Hanriot, Sérgio de Morais, hanriot@pucminas.br
Maia, Cristiana Brasil, cristiana@pucminas.br
Cabezas-Gómez, Luben, luben@pucminas.br
Guzella, Matheus dos Santos, matheusguzella@gmail.com
Cunha, Rodrigo Bruck, rodrigobruckcunha@gmail.com

Pontifical Catholic University of Minas Gerais-PUC-MG, Av. Dom José Gaspar, 500 – Coração Eucarístico - Belo Horizonte, Minas Gerais, Brazil – Cep. 30535-610

Abstract. *In the past years, several wind tunnels are being designed and built to measure aerodynamic forces and moments. It is observed that, even with the recent computational advances, wind tunnels are still an essential tool to the study of the aerodynamics. This paper presents a comparison between experimental and numerical results of velocity and turbulence kinetic energy in the test section of a low speed wind tunnel. Experimental results were obtained through Pitot tube and hot wire anemometry tests and used as boundary conditions for simulations. Numerical results were obtained in ANSYS-CFX 12.1 for two turbulence models: shear stress transport SST models and BSL Reynolds Stress. An analysis of the behavior of velocity and turbulence kinetic energy profiles was done. The comparison between the two turbulence models showed that the model BSL Reynolds Stress presents more detailed airflow characteristics, presenting better results for turbulence kinetic energy. The velocity profiles obtained by both models are very similar.*

Keywords: *wind tunnel, hot wire anemometry, CFD, turbulence kinetic energy*

1. INTRODUCTION

The wind tunnel, in addition to being an important reference in aerodynamics and aeronautical research, can also be applied in simulations that engineers and architects need to predict the development of their projects such as building resistance to winds, the behavior of auto motor vehicles, and to allow the measurement and mapping of displacement and dispersion of pollutants in the atmosphere.

Bady et. al. (2011) and Karava et. al. (2011) reported in their works surveys in wind tunnels, including the assessment of ventilation in buildings. several other studies were performed using wind tunnels: study of the development of secondary instabilities in compressible swept airfoil boundary layers (Liu et al., 2010), study on exhaust gas dispersion from road vehicles (Kandaa et al., 2006a,b), study of the characteristics of the flow in wind turbines (Yu et. al., 2011) and the evaluation of the effect of long-term flights in birds (Jenni-Eiermann et al., 2009).

A method for numerically simulating of the flow conditions in wind tunnels closed circuit was developed by Moonen et. al. (2006). Reliable results are obtained if the wind tunnel is completely modeled and special attention should be paid to the boundary conditions of the CFD model. The numerical model must be validated in a wind tunnel with an empty body and then placed in the test section. The methodology proposed by Moonen et. al (2006) reproduces results in wind tunnels medium speed with an error equal to or below 10%. Offering prospects for future use of this methodology as a tool for design of wind tunnels and testing and validation purposes by CFD technique.

Kulkarni et al. (2011) developed a methodology based on CFD technique about the influence of screens and a circuit subsonic wind tunnel open. Various configurations of honeycombs were simulated and investigations have demonstrated that the best settings are ratio the length and diameter of the cells of the honeycomb is between 8 and 10. For this purpose, the quality of the output stream in the settling chamber is independent of the cell shape of honeycomb. In this study, the authors used the standard RNG k ε turbulence with wall functions in a scalable commercial code, simulations of honeycomb fabric combinations for managing turbulence. The numerical results of various combinations were compared to experimental data and the theoretical results available in the literature. The results confirmed that the proposed methodology may be adopted for all subsections of wind tunnels.

Parente et. al. (2011) proposed one improved k– ε model and wall function formulation a solution for the simulation of Atmospheric Boundary Layer (ABL), that is usually performed using the commercial CFD code with RANS turbulence modeling and standard sand–grain rough wall functions . Such approach generally results in the undesired decay of the velocity and turbulent profiles specified at the domain inlet, before they reach the section of interest within the computational domain. This behavior is a direct consequence of the inconsistency between the fully developed ABL inlet profiles and the wall function formulation. A modified wall function formulation was presented to avoid the over-prediction of the turbulence kinetic energy at the wall. The methodology was implemented and tested on a commercial code and results ensured the homogeneity of the properties on the domain.

Numerical results were obtained using two turbulence models: the shear stress transport (SST) model and the model BSL Reynolds Stress, both implemented into the ANSYS-CFX® 12.1. The numerical simulation was performed at the test section and the results were compared with the experimental data.

2. NUMERICAL METHODOLOGY

Computational Fluid Dynamics (CFD) technique involves numerical solution of the governing flow equations. In the analysis, the solution domain is divided into a large number of infinitesimal control volumes and the governing equations are solved for each of them. In this work, the main governing equations of fluid flow considered were mass and momentum conservation. For turbulent flows, it is necessary to take into account the effects of turbulence. In this paper the effects and turbulence models were considered below (Soares et al., 2009).

2.1 Shear stress transport (*SST*) model

The SST model was proposed by Menter (1994), and grew from the denominated baseline k-ω model which makes use of the k-ε model in regions far away from the walls and the k-ω near the surface. The SST model takes account of the transport of the turbulent shear stress by the limitation of the eddy viscosity, given by Eq. (1):

$$\nu_t = \frac{a_1 k}{\max(a_1 w, SF_2)} \tag{1}$$

Where S are invariational measures of the strain rate and F_2 is a function that creates a restriction for the boundary layer (ANSYS, 2009), calculated by Eq. (2):

$$F_2 = \tanh\left[\left(\max\left(\frac{2\sqrt{k}}{\beta' \omega y'}, \frac{500\nu}{y^2\omega}\right)\right)^2\right] \tag{2}$$

The turbulent kinetic energy, k and turbulent frequency, ω are computed by the following relations:

$$\frac{\partial(\rho k)}{\partial t} + \vec{\nabla}\cdot(\rho U k) = \vec{\nabla}\cdot\left[\left(\mu + \frac{\mu_t}{\sigma_{k3}}\right)\vec{\nabla} k\right] + P_k - \beta' \rho k\omega \tag{3}$$

$$\frac{\partial(\rho \omega)}{\partial t} + \vec{\nabla}\cdot(\rho U \omega) = \vec{\nabla}\cdot\left[\left(\mu + \frac{\mu_t}{\sigma_{\omega 3}}\right)\vec{\nabla}\omega\right] + (1-F_2)2\rho\frac{1}{\sigma_{\omega 2}\omega}\vec{\nabla}k\vec{\nabla}\omega + \alpha_3\frac{\omega}{k}P_k - \beta_3\rho\omega^2 \tag{4}$$

The constants used in this model are, according to ANSYS (2009):

$\beta' = 0.09;\ \alpha_1 = 5/9;\ \beta_1 = 0.075;\ \sigma_{k1} = 2;\ \sigma_{\omega 1} = 2;$

$\alpha_2 = 0.44;\ \beta_2 = 0.0828;\ \sigma_{k2} = 1;$ and $\sigma_{w2} = 1/0.856$

2.2 Reynolds Stress Turbulence (*BSL*) model

The Reynolds Stress Turbulence model is based on formulation of transport equations for all components of the Reynolds stress tensor and dissipation rate. The eddy viscosity concept is not used, and it is solved an equation for the transport of Reynolds stresses. The model uses a differential equation for the Reynolds stress transport computation, based on the turbulence frequency, which is computed using the baseline *k-*ω model.

In this paper, the modeled equations for the Reynolds Stresses are based on an ω-transformation, as presented in ANSYS (2009), showed in Eq. (5):

$$\frac{\partial\left(\rho\,\tau_{ij}\right)}{\partial t}+\frac{\partial\left(U_k\rho\,\tau_{ij}\right)}{\partial x_k}=-\rho P_{ij}+\frac{2}{3}\beta'\rho\,\omega k\delta_{ij}-\rho\Pi_{ij}+\frac{\partial}{\partial x_k}\left(\left(\mu+\frac{\mu_t}{\sigma^*}\right)\frac{\partial\tau_{ij}}{\partial x_k}\right) \tag{5}$$

The constitutive relation for the pressure tensor is given by Eq. (6):

$$\Pi_{ij}=\beta' C_1\omega\left(\tau_{ij}+\frac{2}{3}k\delta_{ij}\right)-\widehat{\alpha}\left(P_{ij}-\frac{2}{3}P\delta_{ij}\right)-\widehat{\beta}\left(D_{ij}-\frac{2}{3}P\delta_{ij}\right)-\widehat{\gamma}k\left(S_{ij}-\frac{1}{3}S_{kk}\delta_{ij}\right) \tag{6}$$

In this model, the Reynolds tensor is given by:

$$P_{ij}=\tau_{ik}\frac{\partial U_j}{\partial x_k}+\tau_{jk}\frac{\partial U_i}{\partial x_k} \tag{7}$$

The tensor D only differs from the Reynolds tensor in the dot-product indices:

$$D_{ij}=\tau_{ik}\frac{\partial U_k}{\partial x_j}+\tau_{jk}\frac{\partial U_k}{\partial x_i} \tag{8}$$

The turbulent viscosity in the diffusion terms of the balance equations of the Reynolds Stresses equation is computed as in the k-ω model, showed in Eq. (9):

$$\mu_t=\rho\frac{k}{\omega} \tag{9}$$

The model constants are given by:

$$\beta'=0.09;\ \widehat{\alpha}=(8+C_2)/11;\ \widehat{\beta}=(8C_2-2)/11;\ \widehat{\gamma}=(60C_2-4)/55;\ C_1=1.8;C_2=0.52$$

More detailed information about the turbulence models formulation showed in this paper can be seen in ANSYS (2009).

3. EXPERIMENTAL PROCEDURES

The experiments were conducted in the 200 mm wide x 200 mm high x 940 mm long test section of the open wind tunnel shown in Fig. 1. The tests were carried out considering the following rotational speeds: 1800, 2500 and 3200 rpm.

Measurements of velocity using a Pitot tube probe were performed at the test section exit region with the objective to obtain the velocity as described in ISO 3966:2008. The measured points were obtained according to "Log-Tchebycheff Method" (Fig.2). Atmospheric pressure and ambient temperature were measured.

A hot wire anemometer was placed into the centre of the test section (0,0 coordinates) with the objective to evaluate the instantaneous velocity and the turbulent intensity of turbulence of the airflow. In the experiments, the room temperature was kept at 293 $K^{\pm 0.5}$, and the atmospheric pressure at 90.60 $^{\pm 0.06}$ kPa .

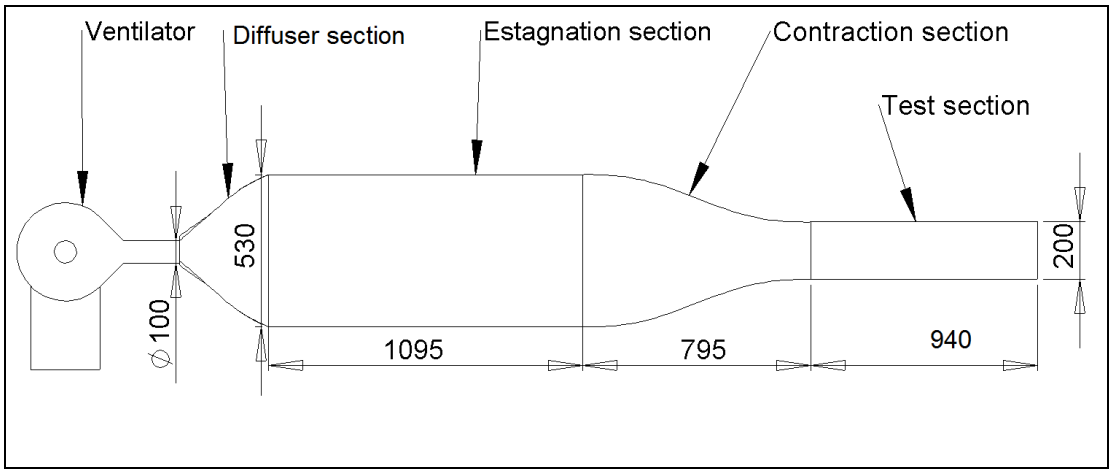

Figure 1. Wind tunnel dimensions.

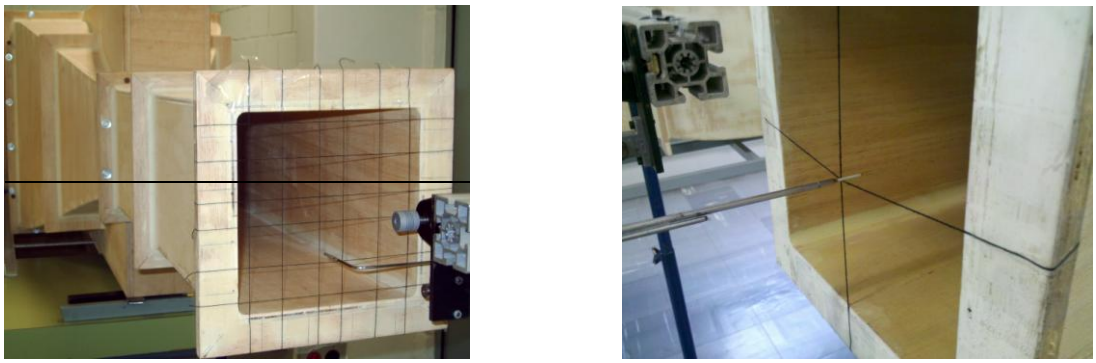

Figure 2 Shows the Pitot tube probe and the hot wire anemometer

4. RESULTS AND DISCUSSIONS

Mass flow rate of 0.2131 kg/s, correspondent to 1800 rpm, obtained from experimental results, was used as inlet boundary condition. For the turbulent variables a medium intensity (5%) of turbulence was adopted. A no-slip boundary condition was considered for the wind tunnel test section walls. The flow was assumed as isothermal with a temperature of 293 K. The outlet boundary condition was set in the code as opening, in order to enable recirculation on the test section exit. The constants at the turbulence models were also assumed as the default values considered in the CFX code (ANSYS, 2009).

As proposed by Menter (2002), in order to characterize both numerical and modeling errors, a hierarchy of three refined meshes has been created. Table 1 presents the quality of the meshes by the min. and max. mesh angles, the max. volume change and Yplus value. Figure 3 shows a cross section of the meshes employed.

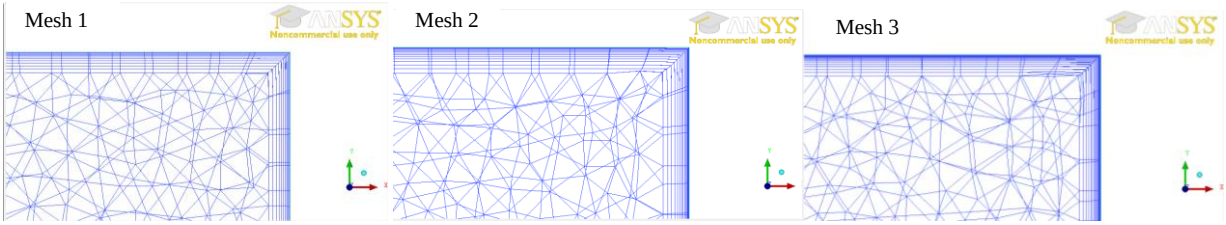

Figure 3. Detailed cross-section of meshes.

Simulations were carried out in an Intel(R) Xeon(R) T3500 Workstation of 2.8Ghz and 12GB of RAM memory. The simulations time for mesh 3, considering both turbulence models, SST and BSL, were 1.97 hours and 4.45 hours, respectively and the numerical results will be presented for this mesh.

Table 1. Main parameters of mesh hierarchy

Mesh	Nodes	Refinement factor	Max y+	Max angle	Min angle	Max volume change
1	299613	-	6.0	146.3	15.4	15.5
2	1204902	4.0	2.6	146.7	13.7	15.1
3	2305783	7.7	0.9	146.7	13.0	11.1

Table 2 shows the velocities mass flow rates experiments with the Pitot tube and hot wire anemometer and temperature constant for rotations 1800, 2500 and 3200 are presented. With the hot wire anemometry system were also calculated the turbulence intensity and the turbulence kinetic energy, according to the methodology proposed by Wilcox (1994). Experimental uncertainties are also presented.

Table 2. Experimental results with the Pitot tube and HWA.

	Pitot tube		Hot wire anemometry			
Rotational speed	Velocity (m/s)	Mass flow rate (kg/s)	Velocity (m/s)	Mass flow rate (kg/s)	Turbulence intensity %	k (m^2/s^2)
1800	$4.57^{\pm 0,07}$	$0.21^{\pm 0,07}$	$5.83^{\pm 0,03}$	$0.23^{\pm 0,03}$	2.71	0.04
2500	$6.32^{\pm 0,04}$	$0.25^{\pm 0,04}$	$7.10^{\pm 0,03}$	$0.28^{\pm 0,03}$	3.24	0.08
3200	$8.03^{\pm 0,02}$	$0.32^{\pm 0,02}$	$7.96^{\pm 0,03}$	$0.32^{\pm 0,03}$	2.41	0.05

Figure 4 presents a comparison between numerical and experimental data for velocity in the central line, in horizontal direction, in the test section of the wind tunnel. It can be noticed good agreement of data. Results obtained by both turbulence models are practically the same, which is an expected behavior.

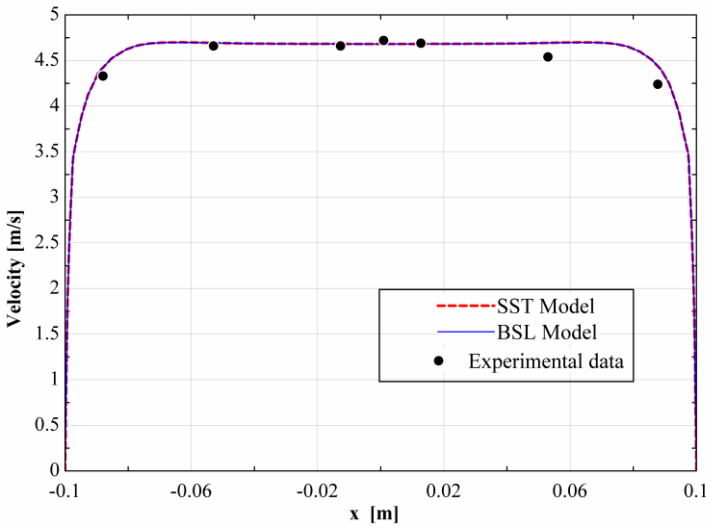

Figure 4. Numerical and experimental velocity data

Figure 5 presents the turbulence kinetic energy profile for mesh 3, considering SST and BSL models. The BSL model predicts greater turbulence intensity values near the walls. The BSL turbulence model computes the Reynolds stresses and gives more detailed values of the computed turbulence quantities, as well as the mean flow variables. However, in order to establish quantitatively which models provides the better profile for the turbulent intensity, the simulation results should be compared with detailed experimental data.

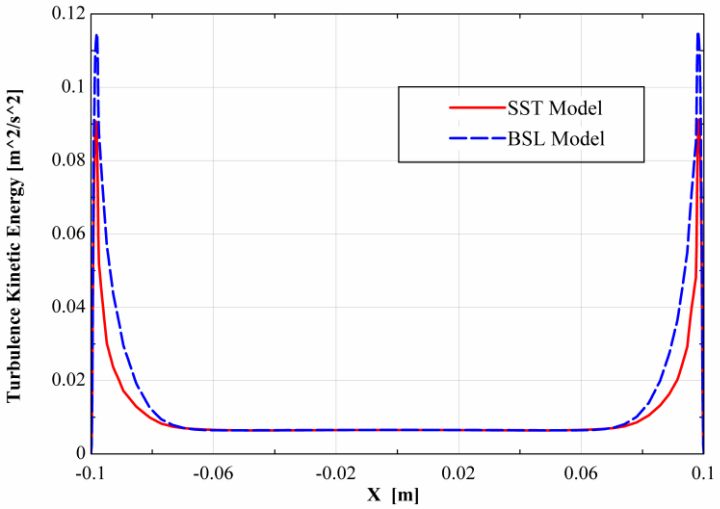

Figure 5. Comparison between turbulence kinetic energy profiles for SST and BSL models.

5. CONCLUSIONS

In the present paper two turbulence models implemented into the ANSYS-CFX® 12.1 software are tested, comparing the obtained simulation results for a test section of a wind tunnel at low speeds with the experimental data. The comparison between the two turbulence models showed that both models present almost the same quantitative behavior for the axial mean velocity, both in very good agreement with the measured experimental data. As BSL models allows the computations of Reynolds Stresses, it is found that this model presents more detailed airflow characteristics, presenting better results for turbulence kinetic energy. More detailed experimental results of the turbulent kinetic energy near the walls are necessary in order to confirm this fact. Considering the above commentaries it is seem that the BSL Reynolds Stress model, implemented into the ANSYS-CFX® 12.1 software, is the best compromise for obtaining a good quality results with a reasonable computational cost.

6. ACKNOWLEDGEMENTS

Authors are grateful to Foundation for the Support of Research of the State of Minas Gerais-Brazil (FAPEMIG), to National Council for Scientific and Technological Development (CNPQ), Federal Center of Technological Education of Minas Gerais (CEFET-MG) and Pontifical Catholic University of Minas Gerais (PUC Minas), who supports this work.

7. REFERENCES

ANSYS, 2009, ANSYS-CFX® Solver Theory manual, Release 12.1.

Bady, M., Kato, S., Takashashi, K., and Huang, H., 2011. " Experimental investigations of the indoor natural ventilation for different building configurations and incidences". Building and Environment, Volume 46, Issue 1, pp. 65-74.

International Organization for Standardization. ISO 3966:2008. Measurement of Fluid Flow in Closed Conduits Velocity Area Method Using Pitot Static Tubes - Second Edition.

Jenni-Eiermann, S., Hasselquist, D., Lindstrom, Å., Koolhaas, A. , and Piersma, T.; 2009. "Are birds stressed during long-term flights? A wind-tunnel study on circulating corticosterone in the red knot". General and Comparative Endocrinology, Volume 164, Issues 2-3, pp. 101-106.

Kandaa, I., Ueharaa, K., Yamaoa, Y., Yoshikawab, Y., and Morikawab, T. ; 2006a. "A wind-tunnel study on exhaust gas dispersion from road vehicles—Part I: Velocity and concentration fields behind single vehicles". Journal of Wind Engineering and Industrial Aerodynamics, Volume 94, pp. 639-658

Kandaa, I., Ueharaa, K., Yamaoa, Y., Yoshikawab, Y., and Morikawab, T.; 2006b. "A wind-tunnel study on exhaust-gas dispersion from road vehicles—Part II: Effect of vehicle queues". Journal of Wind Engineering and Industrial Aerodynamics, Volume 94, pp. 659-673.

Karava, P., Stathopoulos, T., and Athienitis, A.K.; 2011. "Airflow assessment in cross-ventilated buildings with operable façade elements. Building and Environment". Volume 46, Issue 1, pp. 266-279.

Kulkarni, V.; Sahoo N.; Sandip C. D.;2011. "Simulation of Honeycomb-Screen Combinations for Turbulence Management in a Subsonic Wind Tunnel". Journal of Wind Engineering and Industrial Aerodynamics v.99, p.37-45.

Liu, X.P., Niu, J.L., Kwok, K.C.S.,Wang, J.H., and LI, B.Z.; 2010. "Investigation of indoor air pollutant dispersion and cross-contamination around a typical high-rise residential building: wind tunnel tests". Journal of Building and Environment, Volume 45, Issue 8, pp. 1769-1778.

Menter, R. F.; 1994. "Two-equation Eddy-viscosity Turbulence Models for Engineering Applications". *AIAA Journal*. 32(8):269-289.

Menter, R.F.; 2002. "CFD best practice guidelines for CFD code validation for reactor safety applications", EC Project ECORA, Report EVOL-ECORA-D01, pp. 1–47.

Moonen, P.; Blocken, B.; Roels, S.; Carmeliet, J.; 2006, "Numerical modeling of the flow conditions in a closed-circuit low-speed wind tunnel". Journal of Wind Engineering and Industrial Aerodynamics pp. 699–723.

Parente, A., Gorlé, C., Van Beeck, J., Benocci, C., 2011. "Improved k- model and wall function formulation for the RANS simulation of ABL flows". Journal of Wind Engineering and Industrial Aerodynamics v. 99, p 267-278.

Soares C. B., Hanriot S. M., Maia C. B, Cabezas-Gómez, L.; 2009 " Comparison of Numerical and Experimental Results of the Air Flow in the Test Section of an Open Low Speed Wind Tunnel". COBEM 2009

Wilcox, D.C., 1994. Turbulence Modeling for CFD. DCW Industries, Inc, California, USA.

Yu, G., Shen, X., Zhu, X., and Du, Z.; 2011. "An insight into the separate flow and stall delay 16 for HAWT". Renewable Energy, Volume 36, Issue 1, pp. 69-76.

8. RESPONSIBILITY NOTICE

The authors are the only responsible for the printed material included in this paper.